High brightness and high average current electron sources and their applications

APT seminars, FermiLab

O. Mohsen

Northern Illinois University

December 15, 2020

Outline

Table of Contents

Northern Illinois University

Acknowledgment

I would like to acknowledge the work and help I received from these people of whom without, this work would not be possible.

From NIU: P. Piot, D. Mihalcea, T. Xu, A. Lueangaramwong, S. Valluri, N. Tom, N. Adams. A. McKeown, V. Korampally, I. Salehinia,

---

From FermiLab: R. C. Dhuley, M. I. Geelhoed, J. C. T. Thangaraj.

From ANL: John Power, John Byrd, Jiahang Shao, Mike V Fisher, Jacob Packard, Michael P. Kelly, Troy Bennet Petersen,

---

From SLAC: Cho-Kuen Ng, Liling Xiao, Lixin Ge

Northern Illinois University Fermilab Argonne NATIONAL LABORATORY

Motivation

Northern Illinois University

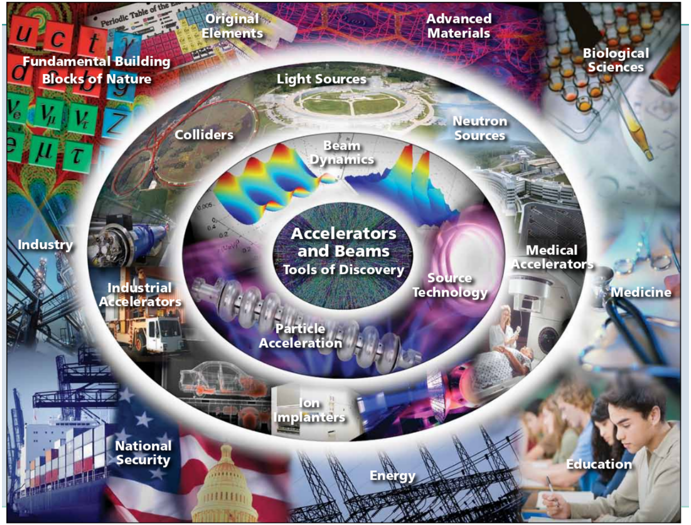

Electron beams

Northern Illinois University

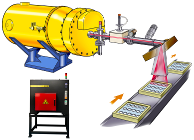

[1]

Food irradiation

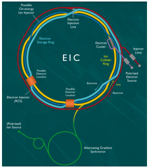

electron ion collider

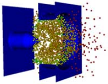

generation of electron beams from nano-tips
https://www.niu.edu/advanced-accelerator-randd

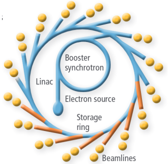

accelerator based light sources
https://simple.wikipedia.org/wiki/Synchrotron

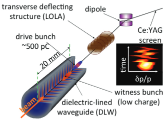

[2]

Advanced Accelerator concept

* †

*https://www.aerial-crt.com/
†https://www.bnl.gov/eic/

Motivation: high brightness electron beams

Northern Illinois University

Brightness is related to the amount of charge in phase-space volume.

$$\boxed{\mathcal{B} \sim \frac{q}{\epsilon_\perp^2 \epsilon_\parallel}}$$

Generation of electron beams using photo-emission followed by acceleration in radio-frequency strucutre

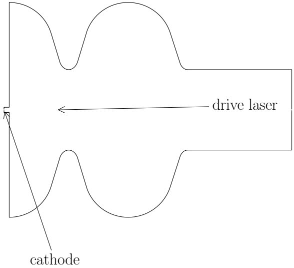

photo emission in RF structure [3]

- The emission is guided by a laser trigger.
- To a first approximation, the emitted particle distribution represents the initial laser pulse.
- Characterised by $QE \sim \frac{\Delta Q/q}{\Delta E/\hbar\omega}$ [4]

Application: brightness

Northern Illinois University

‡

Future Free Electron lasers

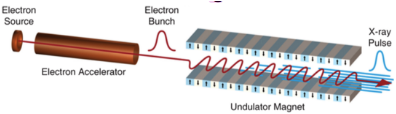

$$\boxed{\rho \sim (\mathcal{B})^{1/3}}$$

$$\boxed{\epsilon_n \lesssim \gamma\beta \frac{\lambda}{4\pi}}$$

This ρ parameter controls the exponential gain length $L_g \sim \rho^{-1}$ and the FEL wavelength λ is set by the electron beam emittance and energy [5, 6].

$$\boxed{Q \sim 100spC,\ \sigma_t \sim 1ps,\ \epsilon_x \sim 100nm}$$

‡http://web.stanford.edu

Ultra fast electron experiments

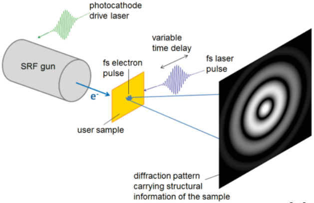

Ultra-Fast electron diffraction setup [7]

Foot-prints accelerator that can provide:

$$\boxed{Q \sim 10sfC,\ \sigma_t \sim 100sfs,\ \epsilon_x \sim 1snm}$$

[8][9].

Motivation: High average current

Northern Illinois University

Generation of electron beams using Field Emission (FE) cathodes:

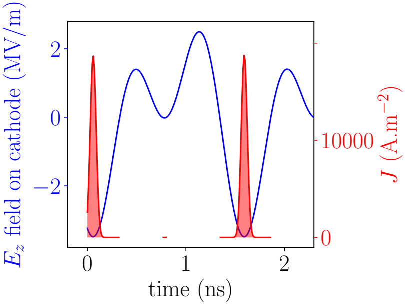

$$j = A(\phi)[\beta_e E]^2 \; e^{\frac{-B(\phi)}{\beta_e E}} \quad [10] \qquad (1)$$

where ϕ is the work function, E is the electric field, β_e is the field-enhancement factor and $A(\phi), B(\phi)$ are constants.

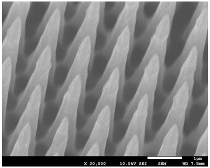

An array of Si nano tips

- Array of nano-tips can be used to enhance the field at the surface
- The emission is solely guided by the applied electric field
- Depends on electric field amplitude and the material

Application: high-average power

Northern Illinois University

High average-power beams

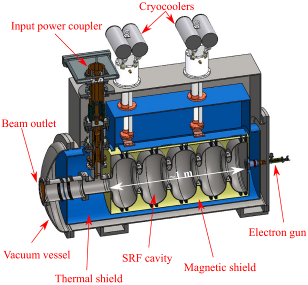

conceptual design of 4.5 cell gun cooled by 2 cryocoolers

The complex infrastructure associated SRF technology is a challenge in applying it outside of research facilities. (e.g. liquefaction and storing of Helium). Recent work in conduction cooling can be the solution [11, 12]

$$\boxed{\mathbf{P} = Q \times f \times \varepsilon} \quad (2)$$

- Many industrial applications require few MeV electron beam with high average power (100s kW) [13, 14].
- Conduction-Cooled SRF systems can provide cooling for up to 4 K.
- Field Emission is an excellent candidate because of its self-gating mechanism and high repetition rate.
- The elimination of the use of a laser-trigger system simplifies the setup a lot.
- When compared to Thermionic Emission, FE makes the SRF-cathode coupling much simpler since it is cold and it does not require insulation
- No back bombardment as in the case of Thermionic.

§

§https://iarc.fnal.gov/

Table of Contents

Northern Illinois University

FE cathodes at NIU

Northern Illinois University

To test FE cathodes, a DC test stand was designed and built at NIU.

- A simple diode configuration setup.
- High voltage applied at the anode.
- Different spacer can be used.
- Scintillating screens with a CCD camera to measure the beam distribution.
- Ultra-high vacuum chamber.
- In-house control system to control and monitor the setup

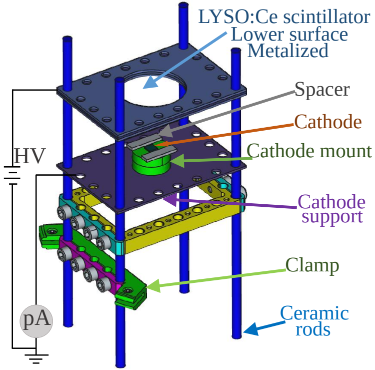

schematic view of the setup courtesy of [15]

Results I

- Cathodes were made by our collaborators at NIU and ANL.
- Different cathodes were made and tested
- Emission from sharp edges around the cathode (dark current)

Self-assembled monolayers of Silica spheres deposited on the Si wafer. The spheres form a mask to structure the wafer via etching processes. A first anisotropic profile is performed with chlorine. A reactive-ion etching process is then achieved using an Ar/SF6 composition of gases to create an isotropic etch profile. Finally, the silicon tips are formed via thermal oxidation;

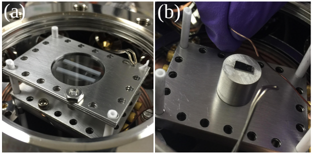

setup at NIU

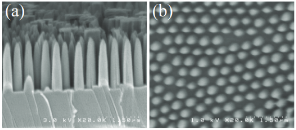

SEM images of Si cathodes

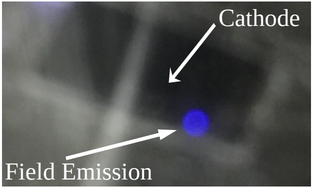

Emission observed from the edges of the cathode

Results II

Northern Illinois University

New spacer and anodes were designed to suppress emission

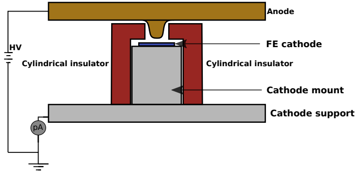

Schematic views of the modified setup to suppress emission from undesired regions.

β: is the field enhancement factor (ratio between how much the field is enhanced due to geometry compared to when it is flat)

F-N current is more explicitly given by: [16]

$$j = A(\phi)[\beta_e E]^2 \; e^{\frac{-B(\phi)}{\beta_e E}} \tag{3}$$

$$I = A \; a \; \phi^{-1} \; 10^{4.52 \frac{1}{\sqrt{\phi}}} \; \beta^2 E^2 \; e^{\frac{-k\phi^{\frac{3}{2}}}{\beta \times E}} \tag{4}$$

where a, k are constants, A (m^2) is the effective emission area.

The common analysis for F-N behaviour is to plot the experimental data in a semi-log plot between $\ln \frac{I}{E^2}$ and $1/E$

$$\boxed{\frac{\ln \frac{I}{E^2}}{1/E} = \ln(\xi A) - \frac{k\phi^{\frac{3}{2}}}{\beta}} \tag{5}$$

Results III

Northern Illinois University

First cathode we successfully tested was Si

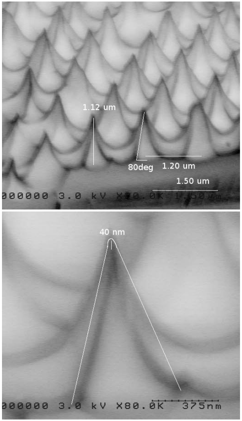

inverted SEM images of the cathode

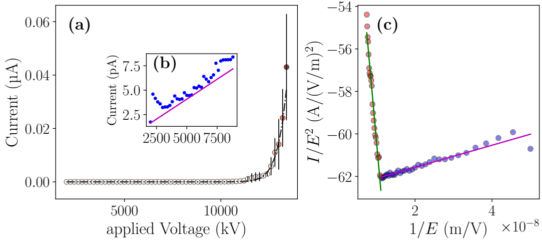

The calculated emitting area A_e and β were low but within our expected values.

$$\boxed{\beta \sim 30}$$

benchmarking β

Northern Illinois University

We use Particle-in-Cell (PIC) code WARP to simulate the geometrical effects of these nano-tips. It could gives us an idea what to expect and we can communicate with the engineering departments on our needs so they can deliver.

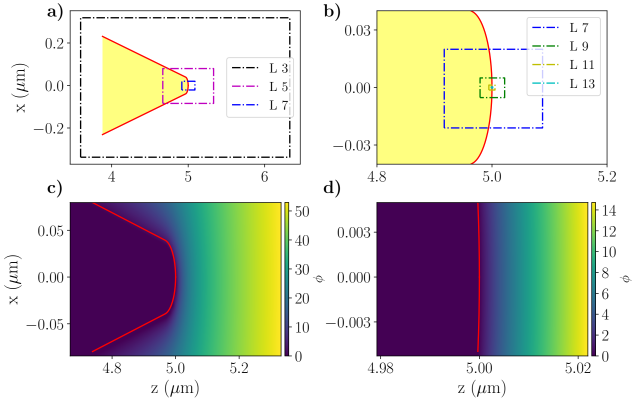

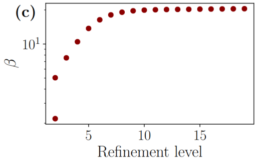

- 20 mesh refinement patches to resolve nm features of the tip
- Final β agrees with what we measured in the lab.

UNCD results (FEA)

Northern Illinois University

Several Si Cathodes were coated with Ultrananocrystalline diamond (UNCD) to test their performances and compare with Si cathode and planar UNCD cathodes (p-UNCD).

- β is attributed to geometrical factors. However, grain boundaries may contribute to higher β
- UNCD has previously shown lower turn on fields and more stable emission when compared to pure Si

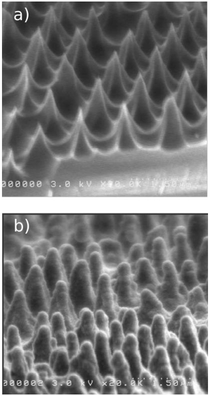

before and after coating with UNCD

UNCD-results

Northern Illinois University

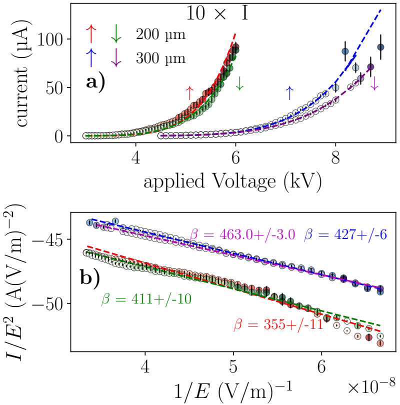

I-V characteristic curve (a) and F-N plot (b)

- The ↑ and the ↓ indicates whether the voltage was increasing or decreasing
- Different spacing were considered (200 µm and 300 µm)
- The current increased by an order of magnitude when the gap spacing was raised from(200 µm to 300 µm) (data for 200 µm was taken first)

p-UNCD

Northern Illinois University

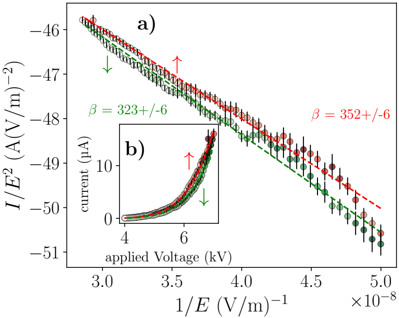

I-V characteristic curve (b) and F-N plot (a)

- Planar-UNCD cathode was also tested
- The test was carried out only 200 µm) because the cathode was damaged

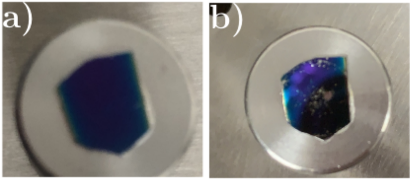

before after

Summary

Northern Illinois University

Table: β and A_e for FEA and planar cathodes.

sample	spacing (µm)	β	A_e 10^{-16} (m^2)
Si ↑	100	27 ± 2	1.2 ± 0.5
FEA ↑	200	355 ± 11 ±109	1.6 ± 0.5 ±0.72
FEA ↓	200	411± 10 ±126	0.31 ± 0.065 ± 0.12
FEA ↑	300	427 ± 6 ± 131	3.2 ± 0.42 ±1.1
FEA ↓	300	463 ± 3 ± 142	1.3 ± 0.07 ± 0.4
planar ↑	200	352 ± 6 ± 108	0.56 ± 0.09 ± 0.19
planar ↓	200	323 ± 6 ± 99	0.96 ± 0.16 ± 0.34

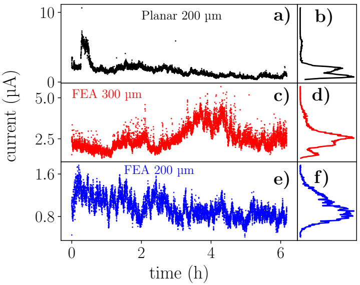

- Higher current for the 300 µm for FEA
- Higher emission area between planar and FEA are purely geometric
- For the same spacing, β is very similar. Comparing with previous bare Si, this indicates that the source of β is mainly due to grain boundaries rather geometric features.

Table of Contents

Northern Illinois University

Conduction cooled electron source

Northern Illinois University

- Based on an elliptical 650-MHz superconducting resonator.
- The cavity is cooled using conduction cooling instead of liquid He.
- Thermal links are made from high purity Aluminium.
- Cylindrical rod is inserted into the cavity
- The rod shifts the eigenmode of the cavity and enhances the field around it (just like a nano tip)

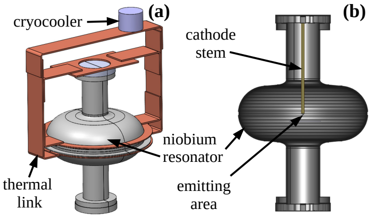

schematic view of the setup

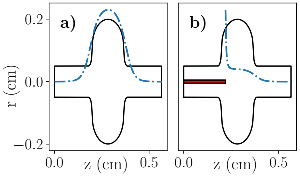

geometry of the nominal and modified cavity

E-source at IARC

Northern Illinois University

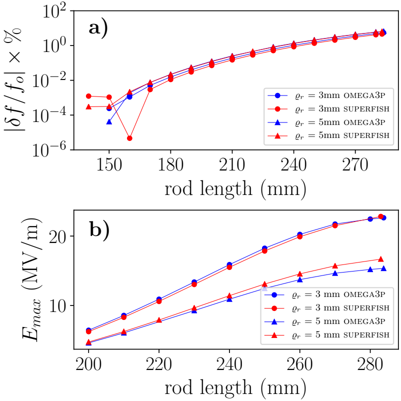

shift in the frequency and peak axial electric field $E_z(r=0)$ for different L_r and ρ_r

- The system is cooled down to cryogenic temperatures by conduction cooling rather than the use of cryogenic fluids.
- Crycooling capacity ranging from 1 - 2 W at $\sim$ 4 K
- Different rod lengths L_r and radius ρ_r were studied
- The field reaches its maximum when the rod is at $L/2$
- Experiential constraints (crycooler and LLRF) had to be met, so a moderate case of $L_r = 22.0$ cm and $\rho_r = 0.5$ was chosen

Dissipated Power

Northern Illinois University

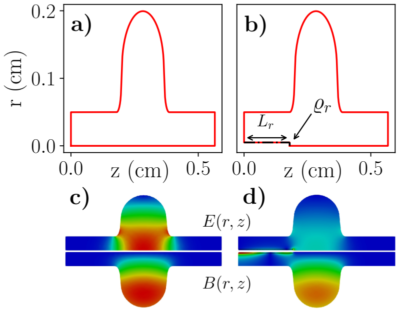

Electric and magnetic field for the nominal and modified cavity

$$\frac{dP}{ds} = \frac{R_s}{2}|\mathbf{H}_{||}|^2$$
$$P = \frac{R_s}{2}\int ds|\mathbf{H}_{||}|^2$$

- The change in the eigen modes introduces higher magnetic flux near the rod and flange.
- In order to make sure that the system stays below critical temperature of Nb, we did thermal analysis of the system on collaboration with the engineering department.
- The thermal model was coupled to the RF simulation via ANSYS

Thermal Analysis

Northern Illinois University

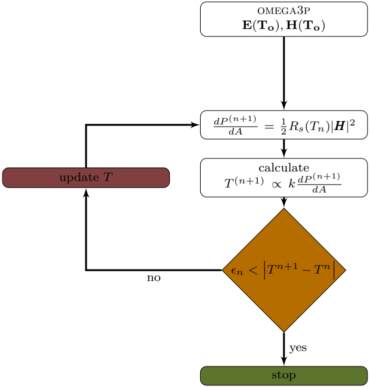

Computational loop for thermal calculations

- Electric and Magnetic fields are calculated based on surface resistance R_s of Nb at 5.0 K using OMEGA3P
- Dissipated power is calculated based on the magnetic fields and normalized to 1.6 Watt (determined by the crycooler)
- Temperature profile T^{n+1} is calculated based on the given dp/ds using ANSYS
- If the difference between initial temperature T^n and T^{n+1} is small $[e_n \sim \mathcal{O}(10^{-2})]$ convergence is reached.

Thermal Analysis II

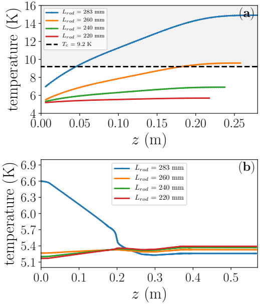

Steady-state temperature reached for various value of rod length L_r along the rod (a) and external cavity wall (b).

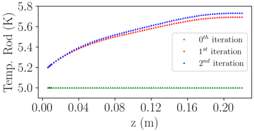

Temperature on the rod vs iteration

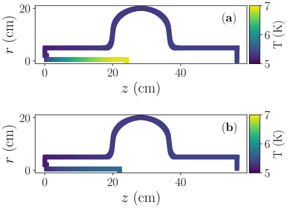

final temperature along the cavity for (a) L_r = 24.0 cm and (b) L_r = 22.0 cm

- Convergence is reached usually after 2 or 3 iterations.
- For cases where $L_r > 24.0$ cm, temperature exceeded T_c
- Highest temperature is at the rod's extremity.

Experimental work I

Northern Illinois University

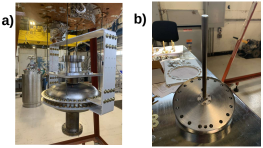

cavity with conduction cooled links (a) and rod with flange (b)

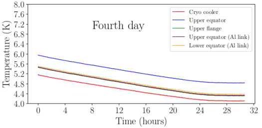

cooling rate vs time (showing only 4th day)

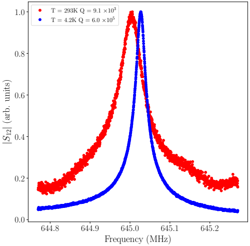

Measured S_{12} before and after cooling

- The setup was assembled and successfully cooled down
- Frequency measured is as expected ± 2 MHz.
- We designed RF coupler with $Q_{ext} \sim 10^8$ to match the excepted Q_o.

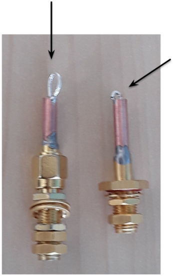

Experimental work II

Northern Illinois University

Table: Temperature comparison between the 2 cool downs

Location	Temp. run I (K)	Temp. run II (K)
Cryocooler port	4.1	4.1
Upper flange	4.8	7.3
Upper Equator	5.0	5.2
Lower Flange	6.9	8.2

$$E_{acc} = \sqrt{Q_2 P_t \left(\frac{R/Q}{L}\right)}[17]$$

$$R/Q = 155.7\Omega$$

- There is a significant temperature difference on the flange (upper mostly)
- During the second cooling, we were able to do RF measurements
- The measured $Q_o \sim 8 \times 10^6 \pm 10^3$ (Expected: $Q_o \sim 10^8$)
- Because the cavity Q_o was lower than anticipated, the Q_{ext} was much higher, this meant we are under-coupled (Forwarded power is mostly reflected and not stored in the cavity).
- The measured $E_{acc} \sim \mathcal{O}(10^{-2})$MV/m (Expected: $E_{acc} \sim 1$ MV/m)
- The issue seems to be the thermal link connection between the thermal links and the upper flange.
- Possible contamination could increase the resistance

Future work

- We are currently warming the cavity and getting ready to do another test before the Holiday.
- a UNCD cathode can be "glued" to the rod extremity.
- WARP was used to simulate emitted current based on previous results.
- Electrons are emitted using F-N equation
- a solenoid can be used at the exist control the beam size
- MHz repetition rate bunches can provide high average power for several applications.

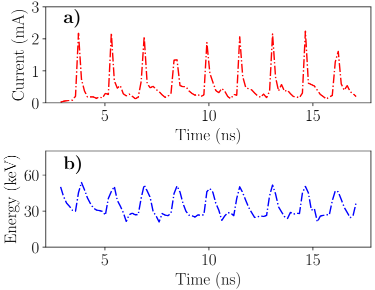

Current and final energy expected to see at the opposite flange

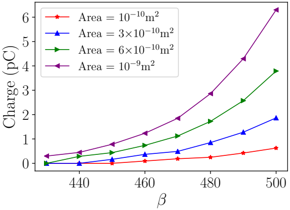

Charge extracted via FE for L_r = 22.0 cm

High-brightness application

Northern Illinois University

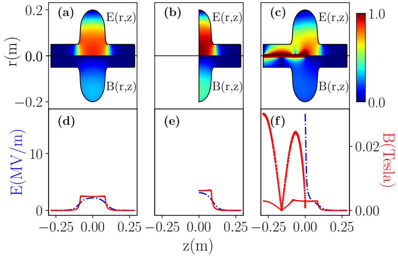

Difference between Full (a) half-model (HC) (b) and rod model (FE) (c)

Table: RF parameters simulated for the three cavity configurations under considerations.

parameter	unit	FC	HC	FE
f	MHz	650	650	607
$\hat{E}_z(r=0)$	MV/m	2.2	3.1	16.9
Q	–	3.12×10^8	3.12×10^8	1.8×10^8

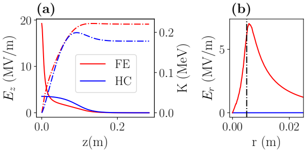

Energy gain (a) and radial field $E_r(r)$ for HC and FE model

- Extending the rod to the center of the cavity gives the maximum E_z for acceleration.
- Comparing to a typical Half cell (HC) geometry from the same cavity the field is x4 times higher
- To keep the cavity under T_c the geometry of the rod needed to change.

High-brightness application

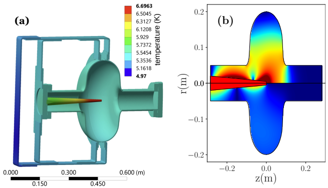

steady state temperature (a) and electromagnetic field (b) for conical rod

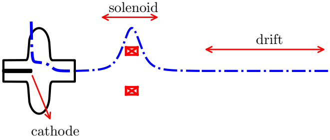

envisioned beamline

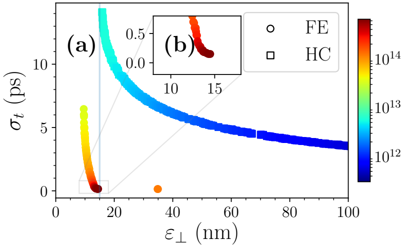

Pareto-Front from the multi-objective optimisation

- Changing the geometry of the rod from a cylindrical to a conical shape help reduce the dp/ds near the flange, which helps in maintaining the cavity under T_c
- Using multi-objective optimisation coupled with beam-dynamics codes IMPACT-T we were able to minimize σ_t and ϵ_x

Summary

Northern Illinois University

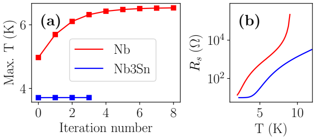

- In terms of beam-dynamics and EM simulations, the model generate ultra-fast electron bunches with superior transverse brightness than typically achieved in a standard half-cell configuration based on a similar elliptical geometry.

- Proof of principle tests are still going and hopefully we will be done before the end of the year.
- The same principle can be applied to an N cells to produce higher energy.
- Using photo-emission to produce low emittance beams and short bunched beams.
- The system can be operated for different cathode configuration to produce electron beams for different applications
- Reducing surface resistance R_s by coating with Nb3Sn could increase the electric field.

Table of Contents

Northern Illinois University

LCLS-II HE: overview

Northern Illinois University

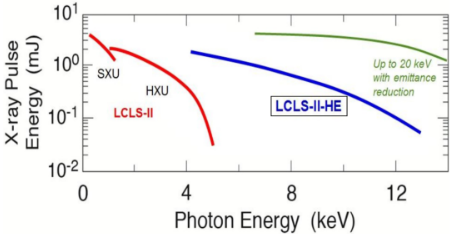

expected increase in photon energy with emittance reduction for LCLS-II HE [18]

	LCLS-II	LCLS-II HE
electron energy (GeV)	4	8
photon energy (keV)	5	13-20

Table: Expected performance for LCLS-II and LCLS-II HE

- The LCLS-II HE is an upgrade to the LCLS-II. It will increase the beam energy up to 8 GeV and photon spectral range up to 12.8 KeV.
- The spectral range can be improved by reducing the emittance of the beam (up to 20 KeV).

Table: Required bunch parameters for the injector of LCLS-II HE

Parameter	Value
Bunch charge	100 pC
ϵ_x	$\leq$ 0.1 µm
σ_z	$\leq$ 1 mm
KE (8 cav)	$\geq$ 90 MeV
σ_p	$\leq$ 200 keV
σ_p (unc)	$\geq$ 5 keV

LCLS-II HE injector modeling

Northern Illinois University

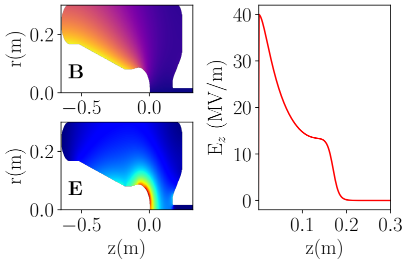

Field map of ANL proposed design (ANL ori) for LCLS-II injector [19]

Table: RC cavity parameters

Parameter	Value
f_o	127 MHz
$E_{cathode}$	40 MV/m

- The design is based on superconducting reentrant-cavity (RC) geometry rather than elliptical $N + 1/2$ gun.
- RC can support sub-GHz frequencies with a reasonable sized cavity.
- Lower frequency operation is beneficial as it relaxes the helium-temperature requirements (e.g. operation at 4.2K is possible instead of 2.7K) ($R_s \sim f^2$))
- Beam dynamics simulation with multi-objective optimisation using ASTRA

example of optimisation

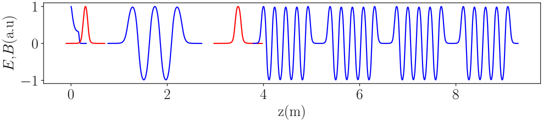

Electric and Magnetic fields along the injector.

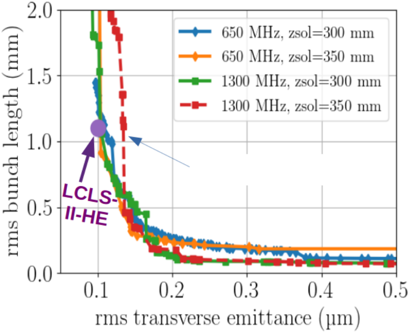

Pareto-Front associated with optimisation of σ_z and ϵ_x for different cases

¶

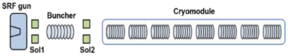

- Initial design was obtained and currently we are working to improve it.
- Different cases for the cavity were simulated using OMEGA3P
- Beam dynamics simulation with multi-objective optimisation using ASTRA

¶courtesy of P.Piot

Optimum Solution: example

Northern Illinois University

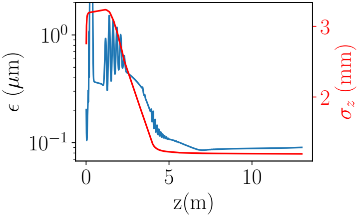

Evolution of σ_z and ϵ_x downstream the injector

Table: Simulation result

Parameter	Value
ϵ_x	0.09 µm rad
EK	45.958 MeV
σ_z	1.2 mm
δ_p^*	9.7 KeV

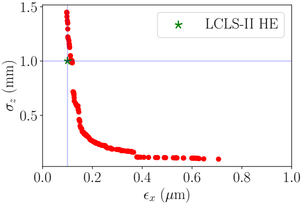

best solution so far was obtained with a 650 MHz buncher and a solenoid as close as possible to the gun (300mm)

- The current design almost meets the LCLS-II HE requirements (for 100 pC, σ_z < 1mm and ϵ_x < 0.1 μm)
- More improvement can be made in focusing solenoid and in the geometry of the cavity
- So far, ellipsoidal initial bunches have been considered.
- Thermal emittance is a big factor in these simulations

Emittance contribution

Northern Illinois University

In photo-injector, (assuming uncorrelated) the emittance can be the sum of different contributions including:

$$\epsilon_n \propto \sqrt{\epsilon_{th}^2 + \epsilon_{rf}^2 + \epsilon_{sc}^2 + \epsilon_{chrom}^2 + \epsilon_{geom}^2}[20]$$

$$\epsilon_{th} = \sigma_x \sqrt{\frac{MTE}{mc^2}}$$

$$\epsilon_{sc} \propto \frac{I}{\alpha}\mu(A), \text{where } \alpha = \frac{eE_o k}{2mc^2}$$

$$\epsilon_{chrom} = \sigma_x^2 \frac{\sigma_p}{mc} K|\sin KL + KL \cos KL|$$

- Thermal emittance is related to the mean transverse energy (MTE) and the laser spot size.
- Minimize the space charge contribution by increase E_o and laser shaping
- minimize the beam size just before the solenoid to reduce Chromatic aberration

More studies: laser pulse

So far in the previous studies, we only considered a uniformly filled ellipsoidal bunch. We are also considering other distribution

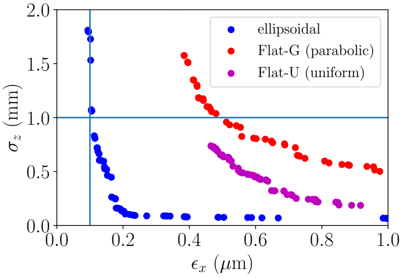

Pareto-Front associated with optimisation with different laser shapes

- Space charge force linearization in ellipsoidal electron bunches can reduce the emittance [21].
- experimental constraints can limit this laser pulse
- Flat-U: plateau distribution in time with a transversely uniform distribution (disk) (cylinder bunch)
- Flat-G: plateau distribution in time with the parabolic transverse radial distribution

More studies: aberration

In order to try to see minimize the effect ϵ_{chrom}, we tried to retract the cathode to introduce E_r:

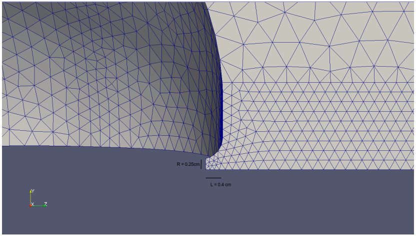

An example of cathode retraction

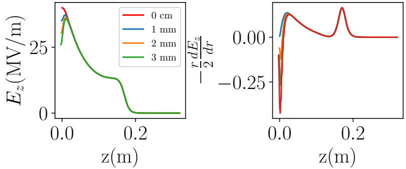

E_z and E_r for different lengths (r=0.75mm)

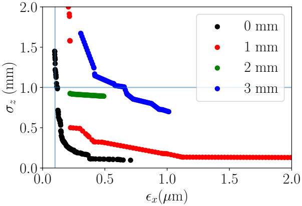

Pareto-Front associated associated with different cathode retraction

- The contribution of the higher field gradient at the cathode is larger than focusing effect from the radial field.

Table of Contents

Northern Illinois University

Conclusion

Northern Illinois University

- FE is a simple and appealing method of extracting electrons for high-average current applications.
- Emission uniformity and robustness of FEA is still an issue.
- The conduction-cooled source was designed and built. Comparing the 2 cooling attempts we had suggest we have an issue with some thermal connection. More attempt before the end of this year.
- In terms of beam-dynamics the conduction-cooled source with the enhanced field, produce brighter beams (order of magnitude) compared to similar geometries with the same dissipated power.
- Injector modeling for the LCLS-II HE is going. Optimisation to include the cavity geometry is undergoing.
- Expanding on the initial design would be to include the e-gun geometry in the optimisation process as well as laser pulse shaping.

Questions?

WIFEL gun

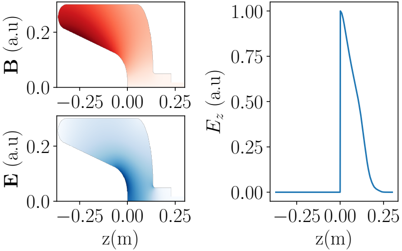

Associated E and B for the WiFEL gun

WiFEL gun being unpacked at ANL

- Transported from SLAC to ANL (currently at ANL)
- can support a low-frequency (sub-GHz) fundamental mode with a reasonably-sized cavity
- Low-frequency operation is beneficial as it relaxes the helium-temperature requirements
- High repetition rate (sub MHz)
- The cavity was tested previously with E_z 20 MV/m

WiFEL gun

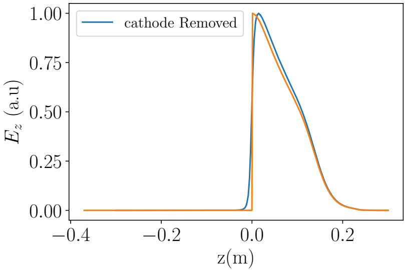

axial electric field E_z when the cathode is removed

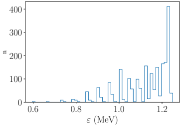

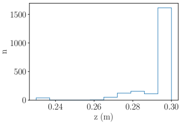

- Currently, the gun is being tested for vacuum leaks.
- Cooling down operation is expected to start next month.
- Testing quality factor Q and V_{acc} is expected without the cathode.
- Dark current studies suggest that emitted electrons will not survive to the exist of the gun.
- X-ray and Gamma-ray detectors will be used to infer the photon energy to the electron energy.

Bibliography I

Northern Illinois University

[1] Suresh D Pillai and Shima Shayanfar. Electron beam technology and other irradiation technology applications in the food industry. In *Applications of Radiation Chemistry in the Fields of Industry, Biotechnology and Environment*, pages 249–268. Springer, 2017.

[2] F Lemery, P Piot, C Behrens, C Gerth, D Mihalcea, C Palmer, J Osterhoff, B Schmidt, and P Stoltz. Progress toward a high-transformer-ratio dielectric-wakefield experiment at flash. *Proc. of IPAC2012, New Orleans, USA*, pages 2166–2168, 2012.

[3] Andre Arnold and J Teichert. Overview on superconducting photoinjectors. *Physical Review Special Topics-Accelerators and Beams*, 14(2):024801, 2011.

[4] Kevin L Jensen. *Introduction to the physics of electron emission*. John Wiley & Sons, 2017.

[5] Zhirong Huang and Kwang-Je Kim. Review of x-ray free-electron laser theory. *Physical Review Special Topics-Accelerators and Beams*, 10(3):034801, 2007.

[6] JB Rosenzweig, N Majernik, RR Robles, G Andonian, O Camacho, A Fukasawa, A Kogar, G Lawler, Jianwei Miao, P Musumeci, et al. An ultra-compact x-ray free-electron laser. *New Journal of Physics*, 22(9):093067, 2020.

[7] Eva Panofski. *Beam Dynamics and Limits for High Brightness, High Average Current Superconducting Radiofrequency (SRF) Photoinjectors*. PhD thesis, Humboldt-Universität zu Berlin, Mathematisch-Naturwissenschaftliche Fakultät, 2019.

[8] Christopher M Pierce, Matthew B Andorf, Edmond Lu, Matthew Gordon, Young-Kee Kim, Colwyn Gulliford, Ivan V Bazarov, Jared M Maxson, Nora P Norvell, Bruce M Dunham, et al. The role of low intrinsic emittance in modern photoinjector brightness. *arXiv preprint arXiv:2004.08034*, 2020.

[9] Jared Maxson, David Cesar, Giacomo Calmasini, Alexander Ody, Pietro Musumeci, and David Alesini. Direct measurement of sub-10 fs relativistic electron beams with ultralow emittance. *Physical review letters*, 118(15):154802, 2017.

[10] Ralph Howard Fowler and L Nordheim. Electron emission in intense electric fields. In *Proc. Roy. Soc. London A*, volume 119, pages 173–181. The Royal Society, 1928.

Bibliography II

Northern Illinois University

[11] R. C. Dhuley, R. Kostin, O. Prokofiev, M. I. Geelhoed, T. H. Nicol, S. Posen, J. C. T. Thangaraj, T. K. Kroc, and R. D. Kephart. Thermal link design for conduction cooling of srf cavities using cryocoolers. *IEEE Transactions on Applied Superconductivity*, 29(5):1–5, 2019.

[12] RC Dhuley, S Posen, MI Geelhoed, O Prokofiev, and JCT Thangaraj. First demonstration of a cryocooler conduction cooled superconducting radiofrequency cavity operating at practical cw accelerating gradients. *Superconductor Science and Technology*, 33(6):06LT01, 2020.

[13] G Ciovati, J Anderson, B Coriton, J Guo, F Hannon, L Holland, M LeSher, F Marhauser, J Rathke, R Rimmer, et al. Design of a cw, low-energy, high-power superconducting linac for environmental applications. *Physical Review Accelerators and Beams*, 21(9):091601, 2018.

[14] Robert Kephart, B Chase, I Gonin, A Grassellino, S Kazakov, T Khabiboulline, S Nagaitsev, R Pasquinelli, S Posen, O Pronitchev, et al. Srf, compact accelerators for industry & society. *Proceedings of SRF2015, Whistler, BC, Canada*, pages 1467–1469, 2015.

[15] Anusorn Lueangaramwong, Corey Buzzard, Swapan Chattopadhyay, Ralu Divan, Venumadhav Korampally, Osama Mohsen, Philippe Piot, et al. Experimental investigation of field-emission from silicon nano-cone cathodes. In *8th Int. Particle Accelerator Conf.(IPAC'17), Copenhagen, Denmark, 14â 19 May, 2017*, pages 548–550. JACOW, Geneva, Switzerland, 2017.

[16] Alexander Wu Chao, Karl Hubert Mess, Maury Tigner, and Frank Zimmermann. *Handbook of accelerator physics and engineering*. World Scientific, Hackensack,New Jersey,USA, 1999.

[17] O Melnychuk, A Grassellino, and A Romanenko. Error analysis for intrinsic quality factor measurement in superconducting radio frequency resonators. *Review of Scientific Instruments*, 85(12):124705, 2014.

[18] TO Raubenheimer et al. The lcls-ii-he, a high energy upgrade of the lcls-ii. In *60th ICFA Advanced Beam Dynamics Workshop on Future Light Sources*, pages 6–11, 2018.

[19] SV Kustaev, S Belomestnykh, I Ben-Zvi, ZA Conway, MP Kelly, B Mustapha, PN Ostroumov, Q Wu, B Xiao, and W Xu. Design of a superconducting quarter-wave resonator for erhic. Technical report, Brookhaven National Laboratory (BNL), Upton, NY (United States), 2014.

[20] Triveni Rao and David H Dowell. An engineering guide to photoinjectors. *arXiv preprint arXiv:1403.7539*, 2014.

[21] Houjun Qian, James Good, Christian Koschitzki, Mikhail Krasilnikov, Frank Stephan, et al. Beyond uniform ellipsoidal laser shaping for beam brightness improvements at pitz. In *60th ICFA Advanced Beam Dynamics Workshop on Future Light Sources (FLS'18), Shanghai, China, 5-9 March 2018*, pages 146–149. JACOW Publishing, Geneva, Switzerland, 2018.